Electronic Materials Letters, Vol. 6, No. 4 (2010), pp. 201-207
DOI: 10.3365/eml.2010.12.201 Published 31 December 2010

Control of Thermoelectric Properties through the addition of Ag in the $Bi_{0.5}Sb_{1.5}Te_3$Alloy

J .K .Lee,[1,2,*] S. D. Park,[2] B. S. Kim,[2] M. W. Oh,[2] S. H. Cho,[2] B. K. Min,[2] H. W. Lee,[2] and M. H. Kim[1]

[1]School of Nano Advanced Materials Engineering Changwon National University,
9 Sarim-dong, Changwon-si, Gyeongnam 641-773 Korea
[2]AMARL Korea Electrotechnology Research Institute,
28-1 Sungju-dong, Changwon-si, Gyeongnam 641-120 Korea

In this study, the thermoelectric properties of the Ag-doped $Bi_{0.5}Sb_{1.5}Te_3$ compounds were investigated in the temperature range from 323 K to 573 K. Ingots were fabricated by a conventional melting process and the powder crushed from ingots was then sintered using a hot-pressing method. The temperature dependence of the Seebeck coefficient and the electrical conductivity of the Ag-doped $Bi_{0.5}Sb_{1.5}Te_3$compound are characteristic of degenerate semiconductors, which is fairly different from the conventional $Bi_{0.5}Sb_{1.5}Te_3$ compound. The power factor ($\alpha^2\sigma$) of the quaternary compound was larger than that of the ternary, which is mainly due to the increase in the electrical conductivity with doping content of Ag. The thermal conductivity was greater than that of the Ag-free$Bi_{0.5}Sb_{1.5}Te_3$compound in the temperature range from 323 K to 523 K. The lattice thermal conductivity showed low values throughout the temperature range. The maximum value of the dimensionless figure of merit (ZT) of the 0.05 wt. % Ag-doped compound and the ternary alloy were 1.2 at 373 K and 0.88 at 323 K, respectively. Each of the maximum peak ZT shifts to a higher temperature region with increases in the doping content of Ag. This is likely due to the control of the lattice thermal conductivity by the twin structure, which had a nano-ordered layer.

Keywords: thermoelectric properties, $Bi_{0.5}Sb_{1.5}Te_3$, Ag addition, semiconductor, carrier concentration, twin boundary

1. INTRODUCTION

The bismuth-telluride (Bi-Te) compound system is extensively used in practical fields despite the fact that it was developed in the 1950's due to its optimum performance (ZT=1.0) and mechanical properties and due to the fact that the thermoelectric technology is competitive in a low temperature range between at room temperature and roughly 373 K at present.[1,2] Recently, there has been considerable interest in reusing waste heat of roughly ~673 K from automobiles and incinerators by thermoelectric technology.[3] Essentially, not only the telluride system including Pb-Te and Bi-Te compounds but also various materials systems such as skutterudite with ZT > 1 that operate in this temperature range have been discussed in this vein.

As an example, the effects of Ag as a dopant have been of great interest as they relate to telluride systems such as the LAST ($AgPb_mSbTe_{m+2}$) and TAGS $(GeTe)_x$ $(AgSbTe_2)_{100-x}$) systems. From previous works,[4,5] the outstanding thermoelectric performance (ZT~2.2 at 800 K) of LAST-m ($AgPb_mSbTe_{m+2}$) compounds was due to Ag–Sb–rich 'nanodots' which caused phonon scattering in the Pb-Te matrix,[4,5] which also developed in the TAGS-85 ($(GeTe)_x$ $(AgSbTe_2)_{100-x}$: TAGS-x)) and the TAGS-80 compounds with ZT=1.5 and 1.7, respectively.[6-10]

Unlike the above results, Shelimova *et al.*[11] reported that limited Ag doping caused an increase of the carrier concentration and improved the power factor in $PbBi_4Te_7$ and $PbSb_2Te_4$ compounds.

In addition, Lošt'á *et al.*[12] reported that the hole concentration increased due to the formation of negatively charged defects ($Ag_{Sb}^{''}$) caused by Ag doping.

Therefore, from previous results, it can be estimated that similar phenomena may develop in the Bi-Te system, as well. Nevertheless, few papers have addressed the effect of Ag doping on the conventional Bi-Te system.

In this work, Ag-doped $Bi_{0.5}Sb_{1.5}Te_3$ compounds were adopted to examine the thermoelectric properties, including the Seebeck coefficient, the electrical resistivity, and the thermal conductivity, in order to determine the effect of Ag doping in the $Bi_{0.5}Sb_{1.5}Te_3$ compound.

2. EXPERIMENTAL DETAILS

The Ag-doped $Bi_{0.5}Sb_{1.5}Te_3$ compounds were fabricated by

*Corresponding author: jackyrhy@keri.re.kr

a melting and hot-pressing method. Each element, Ag, Bi, Sb and Te granules 99.99% in purity, were prepared and mixed. The mixed elements were loaded into quartz tubes and were sealed under an Ar atmosphere. The sealed ampoules were heated to 1233 K for 10 h in a rocking furnace and cooled in air. The melted ingots were crushed by ball milling for 5hrs under an Ar atmosphere. Bulk cylindrical samples (12.7 mm in diameter and 20 mm in thickness) were made by hot pressing under an Ar atmosphere for 30 min at 693 K with a pressure of 200 MPa. A sample was machinedinto a hexahedral piece ($3 \times 3 \times 10$ mm^3) for measurement of the Seebeck coefficient and the electric resistivity, as well as coin pieces(12.7 mm in diameter and 2 mm in thickness) for the measurement of the thermal diffusivity.

The phases of the Ag-doped $Bi_{0.5}Sb_{1.5}Te_3$ compounds were analyzed with an X-ray diffractometer (Philips, X'pert) using $CuK\alpha$radiation ($\lambda = 0.15406$ nm) in the range of 2θ between 20° and 70°. The microstructure and local composition of the ingot were analyzed using an electron microprobe and field emission transmission electron microscopy (FEI, Tecnai G2 F30 S-twin). The thermoelectric properties of the Seebeck coefficient and the electrical resistivity were analyzed by a Z-meter based on the four-probe method (Ulvac-Riko, ZEM-3). The thermal diffusivity was measured by the laser flash method (Netzsch, LFA-447). The heat capacity was obtained by a differential scanning calorimeter (Netzsch, DSC 404C) and the densities of the samples were measured by the Archimedes method. Thethermal conductivity was calculated from the density (d), the heat capacity (C_P), and the thermal diffusivity (a) using the equation = aC_Pd. The carrier concentration was measured by measurement of the Hall effect (ECOPIA, HMS-3000) in an electromagnet of 0.55 T. The electric thermal conductivity (κ_e) and the lattice thermal conductivity (κ_{ph}) were calculated according to the Wiedemann-Franz law ($\kappa_e = L\sigma T$), where L is the Lorenz constant (2.45×10^{-8} V^2/K^2).

3. RESULTS AND DISCUSSION

Figure 1 shows the x-ray diffraction (XRD) pattern of the Ag-doped $Bi_{0.5}Sb_{1.5}Te_3$ compounds. The indexed patterns were defined using the rhombohedral ($R\bar{3}m$) model. All

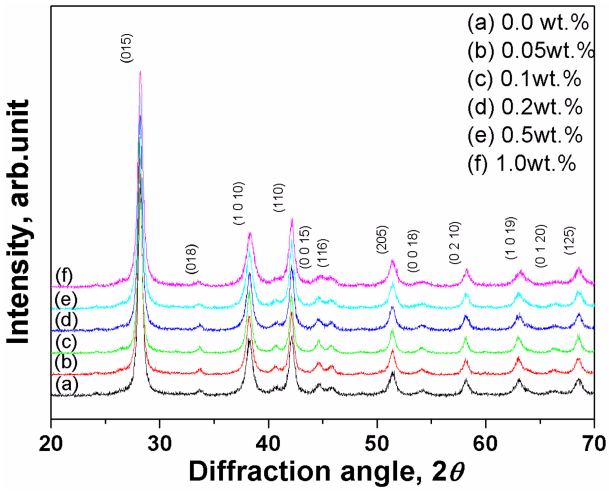

Fig. 1. X-ray diffraction(XRD) pattern analysis of Ag-doped $Bi_{0.5}Sb_{1.5}Te_3$ compounds.

patterns were well matched to that of ternary $Bi_{0.5}Sb_{1.5}Te_3$ compounds. Table 1 shows the defined lattice parameters and the full width at half maximum (FWHM) across the peaks. The decrease of the lattice parameter of the a-axis appears to be negligible. However, the lattice parameter of the c-axis apparently decreases with an addition of Ag. As a result, the volume of the unit cell decreases with the addition of Ag. It should be noted that the atomic radius of Ag is a smaller than that of Bi or Sb ($r_{Bi} = 0.170$ nm, $r_{Sb} = 0.159$ nm and $r_{Ag} = 0.144$ nm).[13] Thus, it may be concluded that the Ag atom can substitute for the Bi or the Sb atom in $Bi_{0.5}Sb_{1.5}Te_3$, which is in good agreement with an earlier report in which Ag could be substituted for Bi or Sb in $Bi_{0.5}Sb_{1.5}Te_3$.[13,14,15] It is unclear why the decrease of the lattice constant was observed only in the c-axis. The XRD-FWHM result was typical, showing that the diffraction peak broadened with the doping content of the Ag. This is related to the crystal quality of the material[16] and is inversely proportional to the crystallite size. The broadening of the diffraction peak is a product of the increased level of polycrystallinity.[17,18]

Figure 2 shows the temperature dependence of the Seebeck coefficient with the doping content of Ag. The Seebeck coefficients were a positive, essentially indicating that the

Table 1. The lattice parameter and XRD-FWHM (2θ) of the Ag-doped $Bi_{0.5}Sb_{1.5}Te_3$ compounds

	Lattice parameter (nm)		Pick position (015)	Cell volume (nm^3)
sample	a	c	FWHM (2θ)	
0	0.4289	3.0468	0.453	0.4854
0.05	0.4289	3.0455	0.449	0.4852
0.1	0.4288	3.0429	0.455	0.4845
0.2	0.4288	3.0429	0.458	0.4845
0.5	0.4287	3.0404	0.467	0.4839
1	0.4285	3.0339	0.497	0.4824

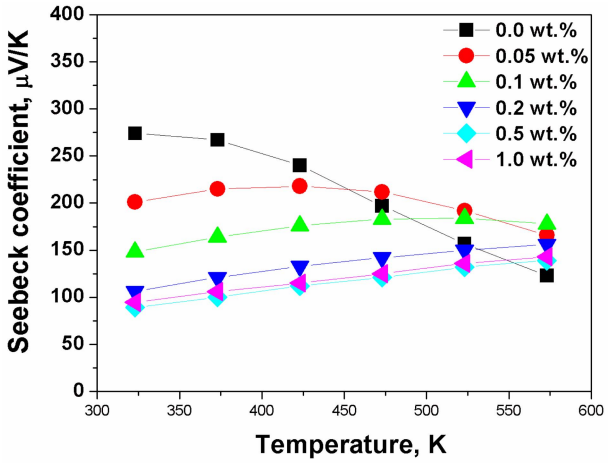

Fig. 2. Temperature dependence of the Seebeck coefficient of Ag-doped $Bi_{0.5}Sb_{1.5}Te_3$ compounds.

major carriers were holes. It was interesting that the Seebeck coefficient of Ag-doped $Bi_{0.5}Sb_{1.5}Te_3$ compounds increasedand then decreased, or increased with the temperature. This is compared to that of Ag-free $Bi_{0.5}Sb_{1.5}Te_3$ compound, in which the Seebeck coefficient decreased monotonously with the temperature.

In the case of the 0.05 wt. % doped compound, the Seebeck coefficient increased up to 427 K and then typically decreased, with the rest showing that with a greater doping content of Ag, the Seebeck coefficient increased with the temperature.

The Seebeck coefficient decreased with the doping content of Ag up to 0.5 wt. % and became saturated at 1 wt. % doping up to 523K. As a result, though the Seebeck coefficient of the Ag-free $Bi_{0.5}Sb_{1.5}Te_3$ compound was higher than that of the Ag-doped $Bi_{0.5}Sb_{1.5}Te_3$ compounds at room temperature, the Seebeck coefficients of the Ag-free $Bi_{0.5}Sb_{1.5}Te_3$ compound were lower than those of Ag-doped $Bi_{0.5}Sb_{1.5}Te_3$ compounds at 573K, in contrast.

It is known that the Seebeck coefficient depends on the electrical state of the conductor, semiconductor and insulator materials. Specifically, the Seebeck coefficient of the conductor shows positive temperature dependence and that of the semiconductor shows negative temperature dependence. Moreover, according to this theory, if a degenerate semiconductor has a medium property between a conductor and a semiconductor, the Seebeck coefficient increases with the temperature up to a specific temperature and then decreases[19] due to the multiband effect,[20] which is caused by the electrons occupying a higher energy state than the Fermi energy level on the Fermi-Dirac distribution due to the temperature increase.[21]

The Seebeck coefficient is related to the carrier concentration.[19,22,23] When assuming a Boltzmann distribution for the holes, the relationship between the Seebeck coefficient and the electrical conductivity at a given temperature can be expressed as follows:[23]

$$\alpha = \frac{k_B}{e}\left[\left(r+\frac{5}{2}\right)+\ln\frac{2(2\pi m^* \kappa_B T)^{3/2}}{nh^3}\right] \quad (1)$$

$$= \frac{k_B}{e}\left[\ln\left(\frac{1}{\sigma}\right)+\ln\mu+r\right]+C1 \quad (2)$$

where m is the effective mass, n is the carrier concentration, h is the Plank's constant, μ is the carrier mobility, and $C1$is the proper constant. From Eq. 2, it can be deduced that the Seebeck coefficient decreases with an increase in the carrier concentration.

Figure 3 shows the temperature dependence of the electrical conductivity in the Ag-doped $Bi_{0.5}Sb_{1.5}Te_3$ compounds together with that of the Ag-free $Bi_{0.5}Sb_{1.5}Te_3$ compound. Typical changes were observed with Ag doping, as shown by the results of Seebeck coefficient changes. As the doping content of the Ag increased, the electrical conductivity of the Ag-doped $Bi_{0.5}Sb_{1.5}Te_3$ compounds increased. This is compared to the result of the Ag-free $Bi_{0.5}Sb_{1.5}Te_3$ compound, which showed a constant value roughly up to 573 K. As is well known, electrical the conductivity depends on the carrier concentration and the carrier mobility according to $\sigma = ne\mu$. Table 2 shows the carrier concentration and the mobility of the Ag-doped $Bi_{0.5}Sb_{1.5}Te_3$ compounds at room temperature. The carrier concentration increased significantly with increases in thedoping content of the Ag. Therefore, the increases in the carrier concentration of the Ag-doped $Bi_{0.5}Sb_{1.5}Te_3$ compounds can be attributed to the increase in the electrical conductivity by Ag doping. Because the defects generated during the substitution of Ag to Bi or Sb factor into the increase in the carrier concentration and electrical conductivity, it is estimated that Ag atoms in the crystal structure of $Bi_{0.5}Sb_{1.5}Te_3$ behave as acceptors.[13]

According to the above results, it is estimated that the

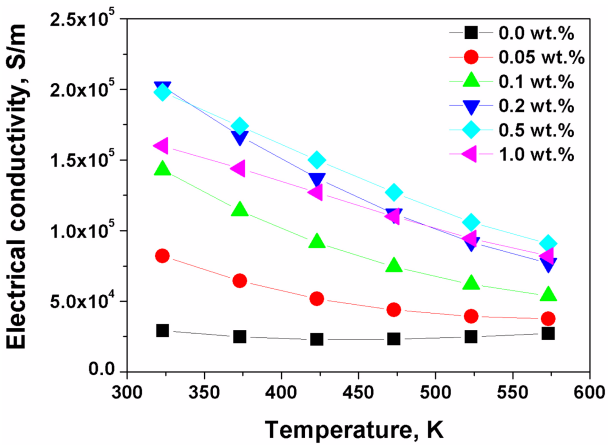

Fig. 3. Temperature dependence of The electrical conductivity of Ag-doped $Bi_{0.5}Sb_{1.5}Te_3$ compounds.

Table 2. The carrier concentration of Ag-doped $Bi_{0.5}Sb_{1.5}Te_3$ compounds

Ag doping Content (wt. %)	Concentration (/cm^3)	Mobility (cm^2/Vs)
0	6.03×10^{18}	3.11×10^2
0.05	2.28×10^{19}	2.65×10^2
0.1	4.76×10^{19}	1.95×10^2
0.2	1.06×10^{20}	1.31×10^2
0.5	1.03×10^{20}	1.36×10^2
1	1.44×10^{20}	8.88×10

typical behavior of the Seebeck coefficient in Ag-doped $Bi_{0.5}Sb_{1.5}Te_3$ compounds is due to the development of metallic behavior owing to the increase in the carrier concentration by Ag doping.

The power factors ($\alpha^2 \times \sigma$) against the temperature are plotted in Fig. 4. The maximum power factor was achieved in the 0.05 wt. % doped compound. The value of the maximum power factor is 3.31×10^{-3}W/m·K^2. The temperature of the maximum power factors on the Ag-doped $Bi_{0.5}Sb_{1.5}Te_3$ compounds shifts higher, specifically with increases in the doping content of Ag. The maximum value is 3.11×10^{-3} at 323 K, 2.44×10^{-3} at 373 K and 1.74×10^{-3} W/m·K^2 at 473 K for the 0.1 wt. %, 0.2 wt. % and 0.5 wt. % doped compounds, respectively.

Figure 5 shows the temperature dependence of the total thermal conductivity on the Ag-doped $Bi_{0.5}Sb_{1.5}Te_3$ compounds. With an increase in the Ag doping content to 0.2 wt. %, the total thermal conductivity of the Ag-doped compounds increased from room temperature to 523 K. Ag-free $Bi_{0.5}Sb_{1.5}Te_3$ compounds with higher than 0.2 wt. % Ag doping showed nearly identical thermal conductivity. With an increase in the temperature, the total thermal conductivity of the Ag-doped $Bi_{0.5}Sb_{1.5}Te_3$ compounds decreased, apart from the 0.05 wt. % Ag doped $Bi_{0.5}Sb_{1.5}Te_3$ compounds in contrast to the Ag-free $Bi_{0.5}Sb_{1.5}Te_3$ compound, which increased with the temperature.

The 0.05 wt. % Ag-doped compound, which showed the maximum power factor of323K in the Ag-doped $Bi_{0.5}Sb_{1.5}Te_3$ compounds, showed the lowest thermal conductivity. In addition, its behavior as regards the temperature was similar to that of the Ag-free $Bi_{0.5}Sb_{1.5}Te_3$ compound. The thermal conductivity of the 0.05 wt. % Ag-doped compound was 0.99 W/m·K at the minimum point of 323 K.

Such behavior of the thermal conductivity of the Ag-doped $Bi_{0.5}Sb_{1.5}Te_3$ compound can be understand by analyzes of the contribution of the lattice thermal conductivity (κ_{Ph}) and the charged thermal conductivity (κ_e) on the total thermal conductivity (κ_{tot}), as shown Fig. 6, and of the microstructures (done by transmission electron microscopy (TEM)) shown in Fig. 7.

The electronic and the lattice thermal conductivity values

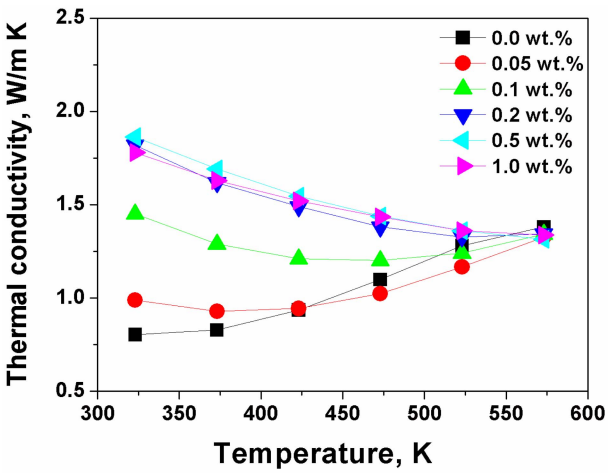

Fig. 5. Temperature dependence of the thermal conductivity of Ag-doped $Bi_{0.5}Sb_{1.5}Te_3$ compounds.

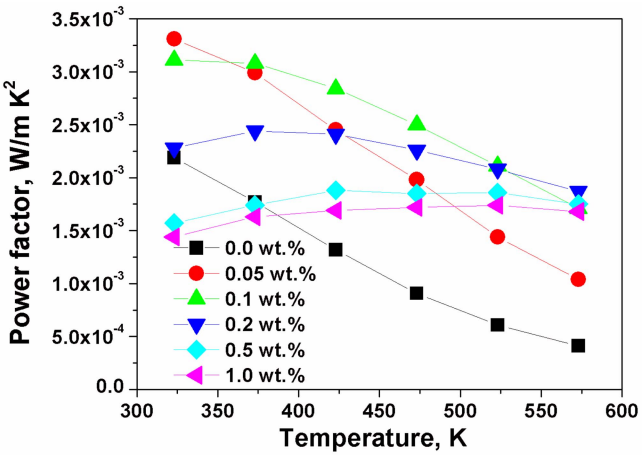

Fig. 4. Temperature dependence of the power factor of Ag-doped $Bi_{0.5}Sb_{1.5}Te_3$ compounds.

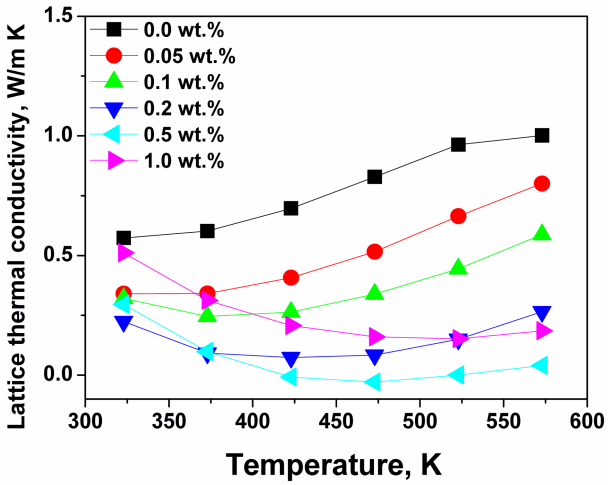

Fig. 6. Temperature dependence of lattice thermal conductivity (κ_{ph}) of Ag-doped $Bi_{0.5}Sb_{1.5}Te_3$ compounds.

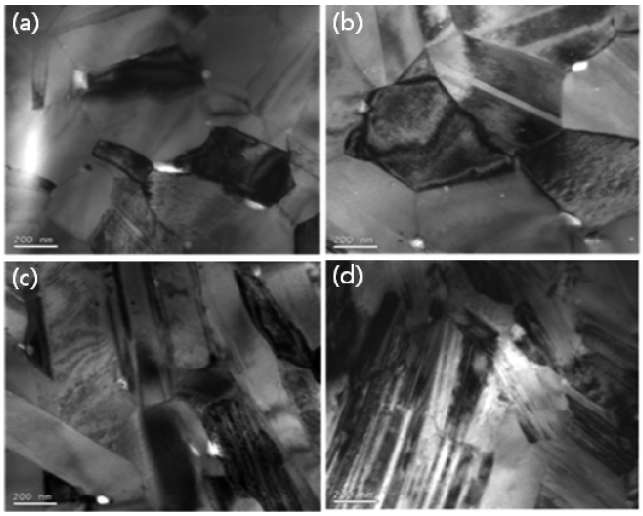

Fig. 7. Transmission electron microscopy (TEM) image obtained in Ag-doped $Bi_{0.5}Sb_{1.5}Te_3$ compound. (a) Ag free, (b) 0.2 wt. % Ag, (c) 0.5 wt. % Ag, (d) 1 wt. % Ag-doped $Bi_{0.5}Sb_{1.5}Te_3$ compound.

were calculated by the Wiedemann-Franz law ($\kappa_e = L\sigma T$; L is the Lorentz constant and T is the absolute temperature) and by $\kappa_{tot} = \kappa_e + \kappa_{ph}$.[20] The value of the Lorentz constant is approximately $\sim 2.45 \times 10^{-8}$ V^2/K^2 ($L = \pi^2/3(k_B/e)^2$) and is constant for metals, while that for semiconductors is dependent on a scattering mechanism ($L = (r+5/2)(k_B/e)^2$, where r is the scattering parameter), ranging from 1.45×10^{-8} to 2.45×10^{-8} V^2/K^2.[24] Although it is difficult to estimate the exact value of the Lorentz constant for a degenerate semiconductor because its value also varies with the any degree of degeneracy, the value of 2.45×10^{-8} V^2/K^2 is adopted for the estimation of κ_e and κ_p. The estimation of κ_e and κ_p with the single value of the Lorentz constant may assist a comparison of the change of the κ_p value with the addition of Ag. Figure 6 shows that the charge thermal conductivity (κ_e) of the Ag-doped $Bi_{0.5}Sb_{1.5}Te_3$ compounds was higher, whereas the lattice thermal conductivity (κ_{ph}) was lower than that of the Ag-free $Bi_{0.5}Sb_{1.5}Te_3$ compound. This indicates that the typical increase in the thermal conductivity of the Ag-doped $Bi_{0.5}Sb_{1.5}Te_3$ compound was mainly influenced by the charge thermal conductivity (κ_e) due to the increase of the charge concentration by Ag doping.

Moreover, the contribution of the charge thermal conductivity (κ_e) decreased and the contribution of the lattice thermal conductivity (κ_{ph}) increased with the temperature, conversely. The total thermal conductivities were nearly identical at a high temperature such as 573 K without Ag doping. However, it was notable that the lattice thermal conductivities of the 0.5 wt. % and 1.0 wt. % Ag-doped $Bi_{0.5}Sb_{1.5}Te_3$ compounds rather decreased and reached constant values despite the fact that the temperature increased. Thus, it can be estimated that other effects acted on the thermal conductivity in the $Bi_{0.5}Sb_{1.5}Te_3$ compounds upon Ag doping.

Figure 7 shows TEM images of that Ag-doped $Bi_{0.5}Sb_{1.5}Te_3$ compound and that Ag-free $Bi_{0.5}Sb_{1.5}Te_3$ compound. A twin structure can be distinctly observed in that Ag-doped $Bi_{0.5}Sb_{1.5}Te_3$ compounds, and they increased with that doping content of Ag. In a detailed analysis, high-resolution transmission electron microscopy (HRTEM) and fast Fourier transform (FFT) analysis were carried out. These results are shown in Fig. 8.

The results confirm that that twin structure has a nanoscale lamellae shape and that the distance between each layer in that twin structure is less than 10nm. In addition, they have the perfect symmetry about that (010) mirror face according to the HRTEM image and the FFT analysis. Klichová *et al.*[13] reported that the four-layer lamellae structure of this type of [$Ag_{0.5}$($Bi_{0.5}$ or $Sb_{0.5}$)]–Te–[$Ag_{0.5}$($Bi_{0.5}$ or $Sb_{0.5}$)]–Te can be combined by Ag doping, which can lead to the creation of a distorted rhombohedral structure.[14] The charge imbalance of Ag^+ and Bi^{3+} or Sb^{3+} causes local distortions.[13,14,15] This indicates that the twin boundary can form as a consequence of the relaxation of the local distortions. Considering the characteristics of twin boundaries which have a coherent phase boundary and several types of nanoscaled morphology, as conformed in the present work, it is

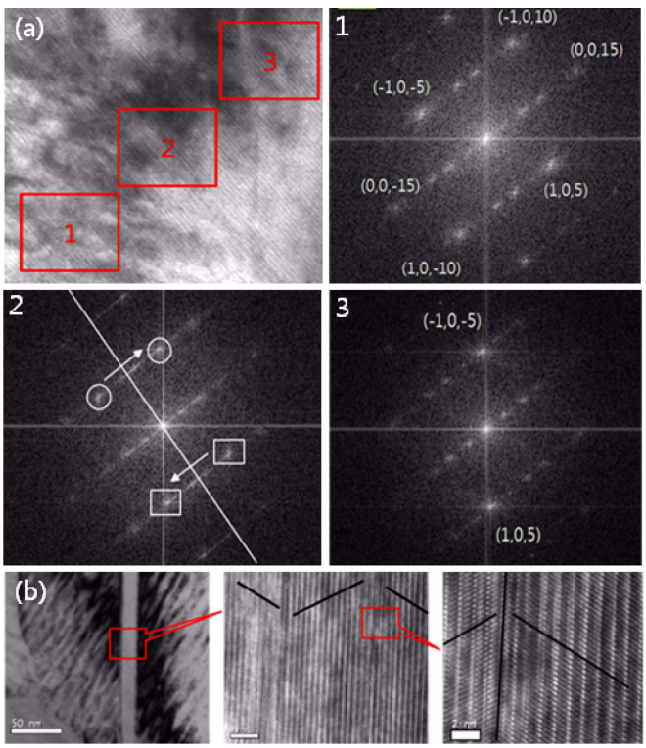

Fig. 8. TEM image analysis of twin boundary. (a) Transmission electron microscopy (TEM) image analysis and diffraction pattern analysis of fast fourier transform (FFT) in (010) face. ; red-marked region 1, 2 and 3 match FFT pattern 1, 2 and 3. (b) High resolution transmission electron microscopy (HRTEM) image obtained in 1 wt. % Ag-doped $Bi_{0.5}Sb_{1.5}Te_3$ compounds.

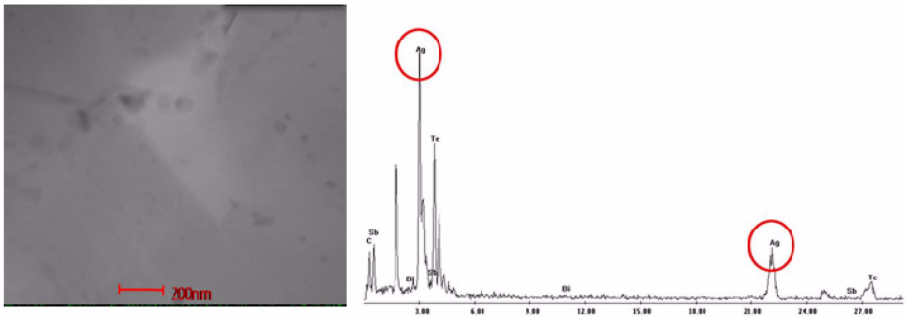

Fig. 9. Scanning transmission electron microscopy (STEM) - energy dispersive spectrometer (EDS) analysis of Ag 1 wt. % doped $Bi_{0.5}Sb_{1.5}Te_3$ compounds.

feasible that the twin boundary could be reduce the lattice thermal conductivity because it acts as a scatter as regards the propagation of phonons.[25] Cao *et al.*[26] reported that a nano scale laminated structure such as the twin boundary in the present work improves the thermoelectric performance by phonon scattering. Consequently, it was considered that the typical behavior of the lattice thermal conductivity in the high Ag-doped $Bi_{0.5}Sb_{1.5}Te_3$ compounds showed low lattice thermal conductivity despite the temperature increase caused by the development of the twin structure.

A scanning transmission electron microscopy (STEM) image of the 1 wt. % Ag-doped $Bi_{0.5}Sb_{1.5}Te_3$ compound is shown in Fig. 9. The precipitates ranged in size from several tens of nanometers to hundreds of nanometers, and the main chemical compositions of the precipitates were Ag and Te. However, nanodots as in the LAST compound system were not observed.

Figure 10 shows the temperature dependence of the *ZT* value in the Ag-doped $Bi_{0.5}Sb_{1.5}Te_3$ compounds and the Ag-free $Bi_{0.5}Sb_{1.5}Te_3$ compound. Compared with the maximum *ZT* of the Ag-free $Bi_{0.5}Sb_{1.5}Te_3$ compound, at 0.88 at 323 K, the maximum *ZT* value was improved by Ag doping. In fact, the maximum *ZT* value of the 0.05 wt. % Ag-doped $Bi_{0.5}Sb_{1.5}Te_3$ compounds was 1.2 at 373 K and, as above mentioned, this resulted from the improvement of the power factordue to the increase in the charged concentration by Ag doping.

In addition, each maximum *ZT* value shifts to a higher temperature region with the doping content of Ag, despite the fact that the maximum *ZT* s decreased somewhat with the temperature; this was estimated to have resulted from the control of the lattice thermal conductivityby the twin structure, which had a nano-ordered layer. This implies that the $Bi_{0.5}Sb_{1.5}Te_3$ compound system can be used in regions of higher temperatures.

4. CONCLUSION

To obtain an improved ZT value, estimations of the values that lead to the formation of a nanostructure or an increase in

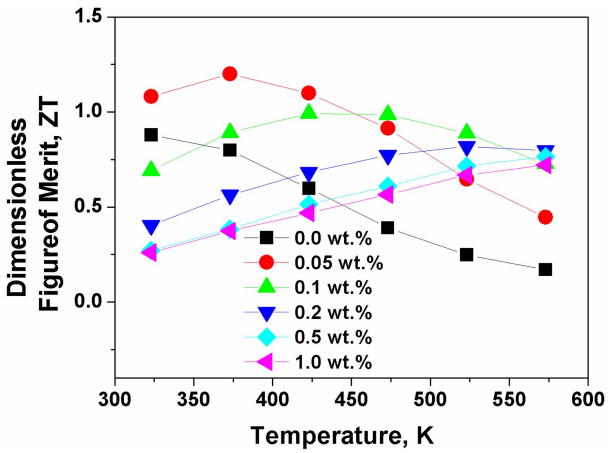

Fig. 10. Temperature dependence of Dimensionless Figure of Merit of Ag-doped $Bi_{0.5}Sb_{1.5}Te_3$ compounds.

the charge carrier concentration with the doping content of Ag in the $Bi_{0.5}Sb_{1.5}Te_3$ compound were made. We confirmed that the twin structure forms with increases in the doping content of Ag in the $Bi_{0.5}Sb_{1.5}Te_3$ compound and that this twin structure acts similar to the nanodot-led phonon scattering. The population of the twin structure of the nanoscale increases with the doping content of the Ag, and the lattice thermal conductivities are minimized. In addition, the carrier concentration increased efficiently with the formation of substitutional defects with the doping content of Ag. Therefore, the power factor was maximized, and the value was determined to be 3.31×10^{-3} W/m·K^2 in the 0.05 wt. % Ag-doped $Bi_{0.5}Sb_{1.5}Te_3$ compound. It was observed that the effects of Ag doping on the thermoelectric properties were optimized in the 0.05 wt. % Ag-doped $Bi_{0.5}Sb_{1.5}Te_3$ compound. The maximum ZT value was determined to be 1.2 at 373 K in this case, while that of the Ag-free $Bi_{0.5}Sb_{1.5}Te_3$ compound was only 0.88. Significantly, each of the maximum peak ZT values shifts to a higher temperature region with an increase in the doping content of the Ag. It was estimated that this was due to the control of the lattice thermal conductivity by the twin structure, which had a nano-ordered layer.

ACKNOWLEDGMENTS

This work was supported by the Energy Efficiency and Resources Program of the Korea Institute of Energy Technology Evaluation and Planning (KETEP) grant funded by the Ministry of Knowledge Economy, Republic of Korea. (No.2008EID11P070000)

REFERENCES

1. A. Majumdar, *Science* **303**, 777 (2004).
2. B. C. Sales, *Science* **295**, 1248 (2002).
3. L. Headings, V. Marano, C. Jaworski, Y. Guezennec, G. Washington, J. P. Heremans, and G. Rizzoni, *Proc. ASME Dynamic Systems and Control Division*, p. 405, American Society of Mechanical Engineers, Chicago, Illinois, USA (2006).
4. K. F. Hsu, S. Loo, F. Guo, W. Chen, J. S. Dyck, C. Uher, T. Hogan, E. K. Polychroniadis, and M. G. Kanatzidis, *Science* **303**, 818 (2004).
5. M. Zhou, J. F. Li, and T. Kita, *J. Am. Chem. Soc.* **130**, 4527 (2008).
6. S. H. Yang, *IOP Sci. Nanotech.* **19**, 245707 (2008).
7. B. A. Cook, M. J. Kramer, X. Wei, and J. L. Harringa, *J. Appl. Phys.* **101**, 053715 (2007).
8. G. Ch. Christakudis, S. K. Plachkova, L. E. Shelimova and E. S. Avilov, *Phys. Status Solidi. A* **128**, 456 (1991).
9. D. M. Rowe, *CRC Handbook of Thermoelectrics*, (ed., D. M. Rowe), p. 267, CRC Press, Boca Raton, FL (1995).
10. H. Wang, J. F. Li, M. Zou, and T. Sui, *Appl. Phys. Lett.* **93**, 202106(2008).
11. L. E. Shelimova, O. G. Karpinskii, T. E. Svechnikova, I. Y. Nikhenzina, E. S. Avilov, M. A. Kretova, and V. S. Zemskov, *Inorg. Mater*. **44**, 371(2008).
12. P. Lošťák, Č. Drasára, J. Horákb, Z. Zhouc, J. S. Dyckd, and C. Uher, *J. Phys. Chem. Solids*, **67**, 1457 (2006).
13. I. Klichová, P. Loš, t'ák, Č. Drašar, J. Navrátil, L. BeneŠ, and J. Šrámková, *Radiat. Eff. Defect. S.* **145**, 245 (1998).
14. L. E. Shelimova, O. G. Karpinskii, P. P. Konstantinov, M. A. Kretova, E. S. Avilov, and V. S. Zemskov, *Inorg. Mater*. **38**, 790 (2002).
15. X. Duan, J. Yang, C. Xiao, and W. Zhu, *Appl. Phys.* **40**, 5971 (2007).
16. M. E. Rodriguez, A. Gutierrez, O. Zelaya-Angel, C. Vazquez, and J. Giraldo, *J. Crystal Growth* **233**, 275 (2001).
17. P. Scherrer, *Nachr. Ges. Wiss. Göttingen* **26**, 98 (1918).
18. J. I. Langford and A. J. C. Wilson, *J. Appl. Cryst*. **11,** 102 (1978).
19. H. S. Dow, M. W. Oh, S. D. Park, B. S. Kim, B. K. Min, H. W. Lee, and D. M. Wee, *J. Appl. Phys*. **105**, 113703 (2009).
20. G. S. Nolas, J. Sharp, and H. J. Goldsmid, *Thermoelectrics: Basic Principles and New Materials Developments*, p. 39, Springer, Berlin (2001).
21. D. Jiles, *Introduction to the Electronic Properties of Material*, p.75, Chapman & Hall Press London (1994).
22. M. W. Oh, D. M. Wee, S. D. Park, B. S. Kim, and H. W. Lee, *Phys. Rev B* **77**, 165119 (2008).
23. S. S. Kim, S. Yamamoto, and T. Aizawa, *J. Alloys Compd*. **375**, 107(2004).
24. J. E. Parrott and A. D. Stukes, *Thermal Conductivity of Solids*, pp. 80-89 (1975).
25. S. H. Yang, T. J. Zhu, S.N. Zhjang, J. J. Shen, and X. B. Zhao, *J. electronic Matt*. (2009).
26. Y. Q. Cao, X. B. Zhao, T. J. Zhu, X. B. Zhang, and J. P. Tu, *Appl. Phys. Lett*. **92**, 143106 (2008).